

# Temperature Dependent Partitioning of C152 in Binary Phosphatidylcholine membranes and Mixed Phosphatidylcholine/Phosphatidylethanolamine Membranes

*Christine A. Gobrogge, Victoria A. Kong, Robert A. Walker\**

## Supporting Information

### CONTENTS

- Differential Scanning Calorimetry
- Time-resolved data analysis
- Melting temperatures
- Time-Resolved Fluorescence
  - DLPC/DMPC mixtures
  - DMPC/DMPE mixtures

### Differential Scanning Calorimetry.

The melting temperature of 20 mM DMPE vesicles (in 10 mM PBS, pH = 7) and 20 mM DMPE vesicles doped with C152 were measured using a TA Instruments Q2000 Differential Scanning Calorimeter (DSC).

Pure buffer references (10 mM PBS) were used for both pure and doped samples. The vesicles were equilibrated well below the melting temperature, after which the temperature was increased at a rate of 1 °C min<sup>-1</sup>. Temperature sensitivity of the Q2000 DSC is ± 0.1 °C. Data were analyzed using TA Instruments Trios software.

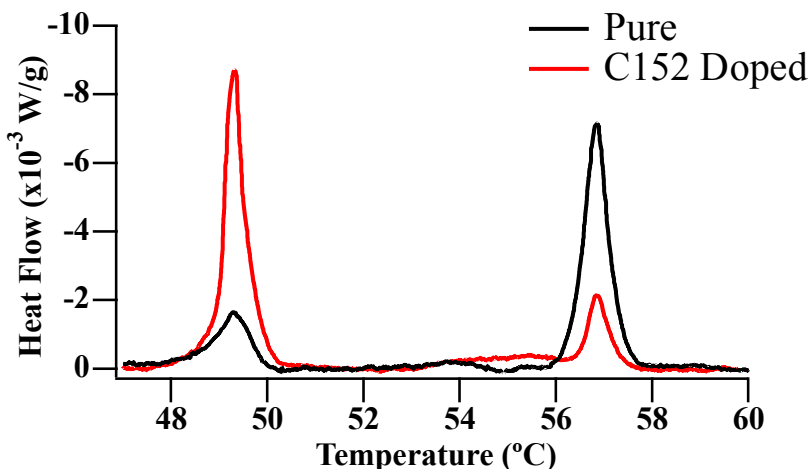


Figure S1. DSC traces of pure DMPE vesicles (black) and DMPE vesicles doped with C152 (red).

### Time-Resolved Data Analysis

The procedure for calculating solute distribution in vesicle solutions is as follows: raw fluorescence data were collected until the fluorescence intensity at time  $t=0$  reached 8,000 counts. Data were fit unconstrained to a sum of exponential functions:

$$I(t) = \int_0^t \text{IRF}(t') \sum_{i=1}^n A_i e^{-\frac{t-t'}{\tau_i}} dt' \quad (1)$$

where  $A_i$  is the amplitude of component  $i$  and  $\tau_i$  is the lifetime of component  $i$ . The quality of fits was initially evaluated by assessing each fit's  $\chi^2$  value. The corrected Akaike Information Criterion (AIC), further described elsewhere,<sup>158</sup> was used to statistically estimate the number of exponential terms ( $n$ ) in Eqn. 1. Typical  $\chi^2$  values ranged from 0.90 to 1.10 when the model accounted for three lifetimes and three associated amplitudes:

$$I(t) = \int_0^t \text{IRF}(t') \left[ A_a e^{-\frac{t-t'}{\tau_a}} + A_b e^{-\frac{t-t'}{\tau_b}} + A_c e^{-\frac{t-t'}{\tau_c}} \right] dt' \quad (2)$$

where  $a$ ,  $b$ , and  $c$  refer to unique solvation environments in a vesicle solution. At any given instant, the fluorescence intensity  $I(t)$  is also equal to the number of excited solutes

in each environment ( $C_i^*(t)$ ) multiplied by the appropriate, solute dependent radiative rate constants ( $k_r$ ):

$$I(t) = C_a^*(t)k_{r,a} + C_b^*(t)k_{r,b} + C_c^*(t)k_{r,c} \quad (3)$$

where  $I(t)$  and  $C_i^*(t)$  are implicitly referenced to a standard state (e.g. 1M). Assuming the three populations are independent of each other and do not interconvert, solutes decay via first order kinetics:

$$C_i^*(t) = C_i^*(0)e^{-(k_{r,i}+k_{nr,i})t} \quad (4)$$

where  $C_i^*(0)$  is the population of excited C152 in environment  $i$  at the moment of excitation. Eqn. 4 may be substituted into the expression for the fluorescence intensity at time  $t$  (Eqn. 3) to arrive at the expanded expression:

$$I(t) = C_a^*(0)k_{r,a}e^{-(k_{r,a}+k_{nr,a})t} + C_b^*(0)k_{r,b}e^{-(k_{r,b}+k_{nr,b})t} + C_c^*(0)k_{r,c}e^{-(k_{r,c}+k_{nr,c})t} \quad (5)$$

At time  $t=0$ , Eqn. 5 simplifies to equal to the sum of the excited state populations multiplied by the relevant radiative rate constants:

$$I(0) = C_a^*(0)k_{r,a} + C_b^*(0)k_{r,b} + C_c^*(0)k_{r,c} \quad (6)$$

Eqn. 1 may also be related to Eqn. 6 to show the relationship between the amplitude associated with component  $i$  ( $A_i$ ) and the excited state concentration of the species in environment  $i$ :

$$A_i = C_i^*(0)k_{r,i} \quad (7)$$

To calculate the distribution of solutes in each environment ( $i$ ), Eqn. 7 clarifies that the amplitudes associated with the solute in environment  $i$  (as provided from Eqn. 1) must be divided by the radiative decay rate of the solute in bulk environment  $i$ , as shown in Eqn.

8:

$$C_i^*(0) = \frac{A_i}{k_{r,i}} \quad (8)$$

Finally, the relative percent of solute in environment  $i$  at the moment of excitation ( $X_i$ ) may be calculated through a simple normalization:

$$X_i = \frac{C_i^*(0)}{C_a^*(0) + C_b^*(0) + C_c^*(0)} = \frac{\frac{A_i}{k_{r,i}}}{\left(\frac{A_a}{k_{r,a}} + \frac{A_b}{k_{r,b}} + \frac{A_c}{k_{r,c}}\right)} \quad (9)$$

where numerical values for  $A_i$  are produced using Eqn. 1 (FluoFit software), and radiative rates are calculated using the fluorescence lifetimes and quantum yields.

An important point to note is that the analysis of C152 decay traces in vesicle containing solutions required several assumptions. First, we assumed that the lifetimes that resulted from fitting the data that corresponds to C152 sampling solvation environments corresponding to different bulk solution limits. Such action seemed reasonable given that unconstrained fitting of each decay consistently resulted in three lifetimes: one short, sub-ns lifetime ( $\tau_1$ ), one intermediate lifetime ( $\tau_2$ ) that shortened from  $\sim 2.4$  ns at low temperatures to  $\sim 1.0$  ns at higher temperatures and one long lifetime of  $\sim 4.5$  ns ( $\tau_3$ ). The short lifetime matched exactly the lifetime of C152 in bulk aqueous buffer and was assigned to solutes that remained unassociated with lipid vesicles. The intermediate lifetime at low temperatures corresponded to C152 in polar aprotic solvents (such as acetonitrile) and at higher temperatures (when lipid bilayers were in their fluid, liquid crystalline state), the  $\sim 1.0$  ns lifetime corresponded to C152 in polar protic solvents (such as methanol).

Correspondingly, this intermediate lifetime ( $\tau_2$ ) was assigned to C152 solutes solvated in the polar headgroup and glycerol backbone regions of the lipid bilayer, and the

shift from polar aprotic to polar protic solvation was attributed to water permeation into this region at temperatures above the gel-liquid crystalline transition temperature. The long lifetime ( $\sim 4.5$  ns) is markedly longer than C152's lifetime in alkanes ( $\sim 3.5$  ns), but given that the nonpolar environment in lipid membranes is only  $\sim 3$  nm wide and solvation is constrained by long, ordered acyl chains, one might reasonably expect that C152's lifetime will be lengthened in such confinement.<sup>159,160</sup> Consequently, this third lifetime is assigned to C152 sampling the nonpolar, alkane like environment lipid bilayer. We also assume that the radiative rates of C152 in vesicle containing solutions correspond to the radiative rates of C152 in their assigned bulk solvation environment.

The method of analysis described in Eqns 18 also requires the assumption that the equilibrium distribution of C152 solutes prior to excitation does not change during an experiment (i.e. solutes do not move from one environment to the other following excitation). Finally, we assumed that the bulk solution solvation mechanisms (e.g. twisted intramolecular charge transfer (TICT) state formation) remained accurate for the heterogeneous solvation environments sampled by solutes in vesicle containing solutions.

## Reduced Temperatures

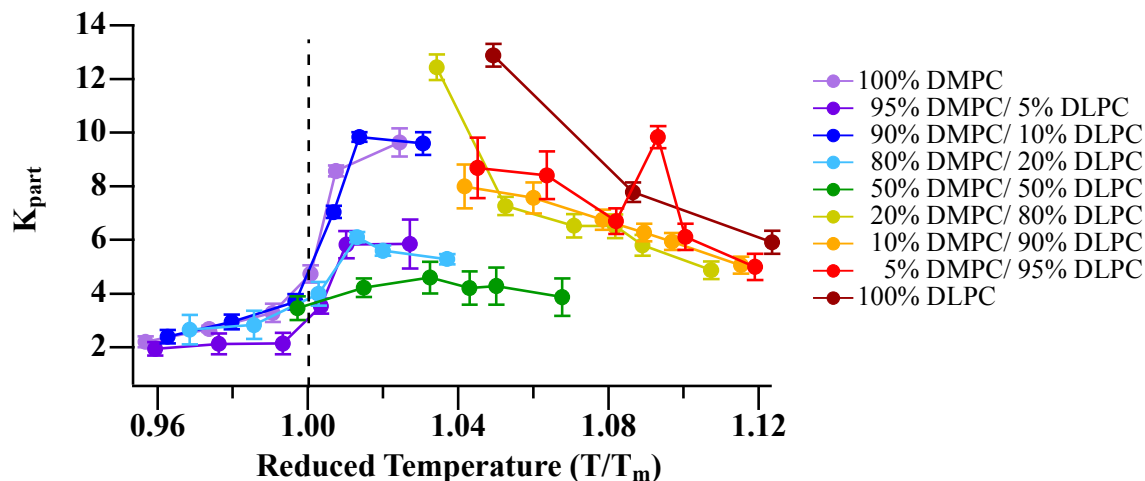


Figure S2. Partition coefficient ( $(A_2 + A_3)/A_1$ ) of C152 in mixed DLPC/DMPC vesicles.

## Melting Temperatures

Table S1. Melting temperatures of 20 mM DLPC/DMPC vesicles.

Mole Ratio DMPC: DLPC	$T_m$ (°C)	$T_{m, ideal}$ (°C)*
0:100	-3.3	-3.3
1:99	-3.1	-2.5
5:95	-2.2	0.4
10:90	-1.3	3.3
20:80	0.7	7.8
50:50	7.3-14.9	16.0
80:20	16.4-20.5	20.7
90:10	19.4-22.1	21.9
95:5	22.0	22.3
99:1	22.5	22.7
100:0	22.8	22.8

\* The ideal melting temperatures were derived from the calculated transition curves discussed in the text.

Table S2. Melting temperatures of 20 mM DMPE/DMPC vesicles.

Mole Ratio DMPE: DMPC	$T_m$ (°C)	$T_{m, ideal}$ (°C)*
0:100	22.8	22.8

1:99	23.0	24.2
5:95	23.0	25.4
10:90	23.2	26.7
20:80	25.5-30.8	29.2
50:50	33.0-40.6	36.7
80:20	44.8-47.9	43.9
90:10	46.3-49.8	45.9
95:5	49.1	48.1
99:1	49.3	49.3
100:0	56.3*	49.5

\* The ideal melting temperatures were derived from the calculated transition curves discussed in the text.

## Time Resolved Fluorescence

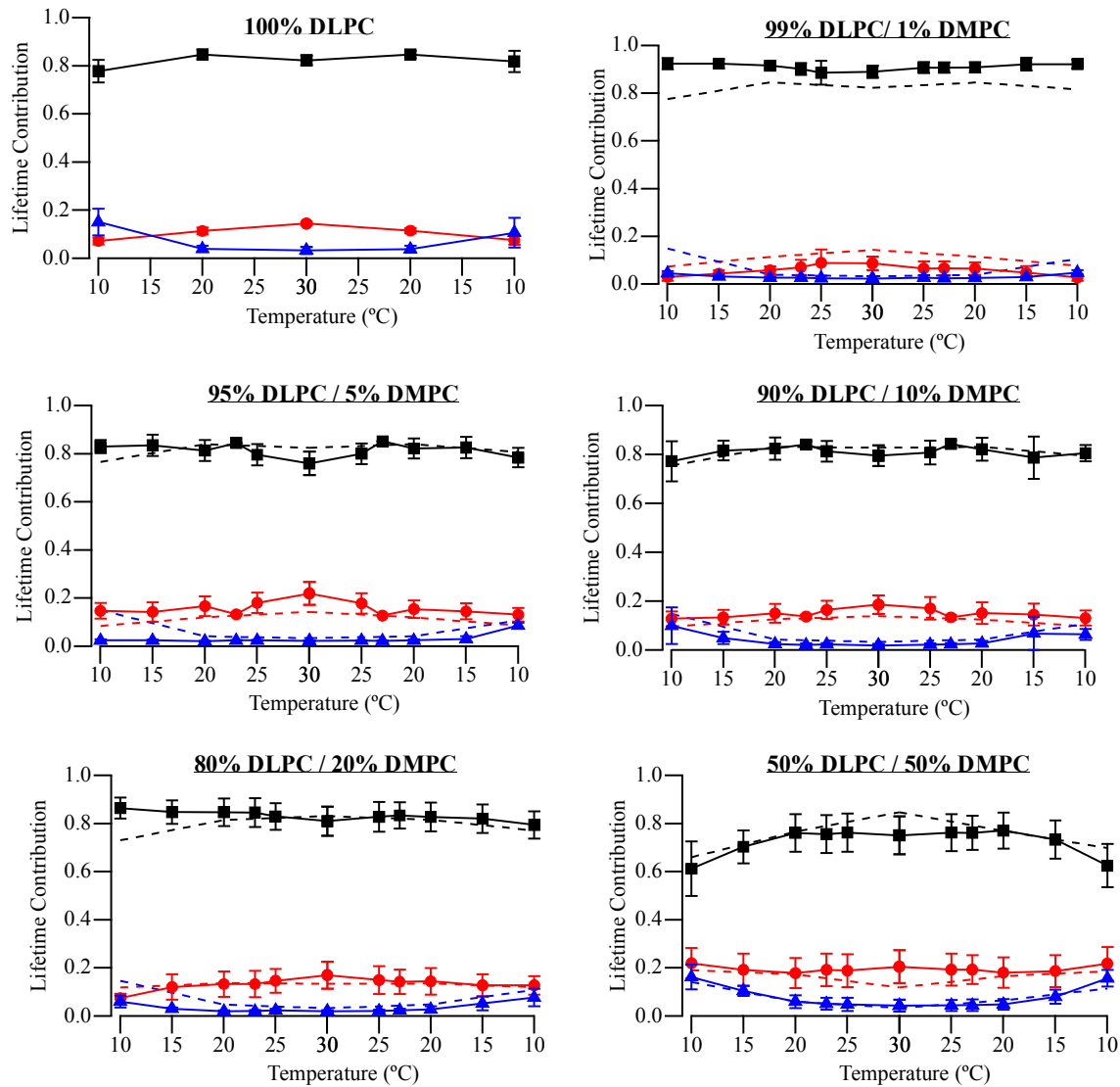


Figure S3. Lifetime contribution of C12 in buffer (red circles), polar (black squares), and nonpolar (blue triangles) environments in vesicles composed of pure DLPC (top left), 99% DLPC/ 1% DMPC (top right), 95% DLPC/ 5% DMPC (middle left), 90% DLPC/ 10% DMPC (middle right), 80% DLPC/ 20% DMPC (bottom left), and 50% DLPC/ 50% DMPC (bottom right).

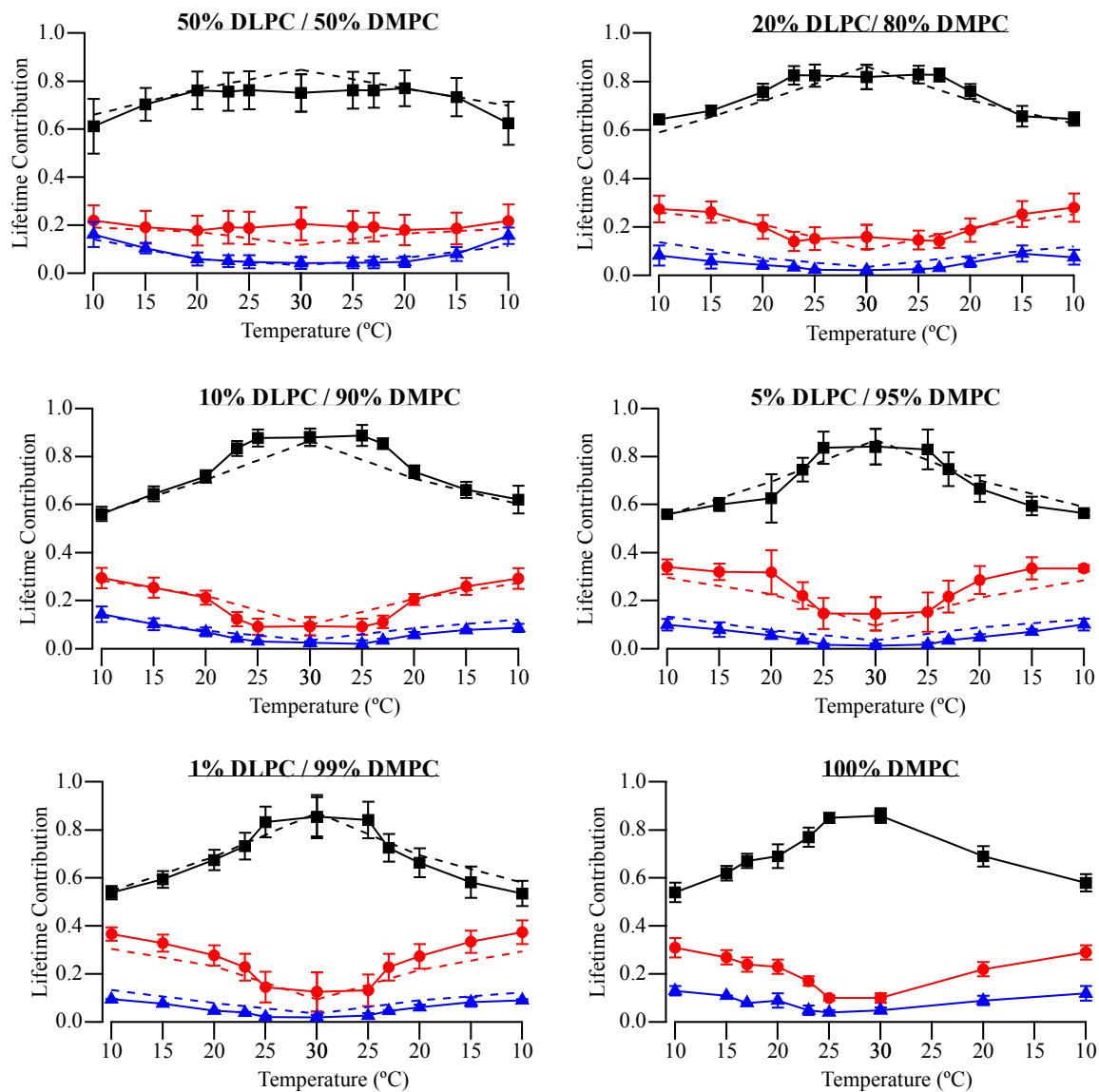


Figure S4. Lifetime contribution of C152 in buffer (red circles), polar (black squares), and nonpolar (blue triangles) environments in vesicles composed of DMPC enriched vesicles: 50% DMPC / 50% DLPC (top left; equimolar concentration is reshown here for comparison purposes), 80% DMPC, 20% DLPC (top right), 90% DMPC/ 10% DLPC (middle left), 95% DMPC/ 5% DLPC (middle right), 99% DMPC/ 1% DLPC (bottom left), and pure DMPC (bottom right).

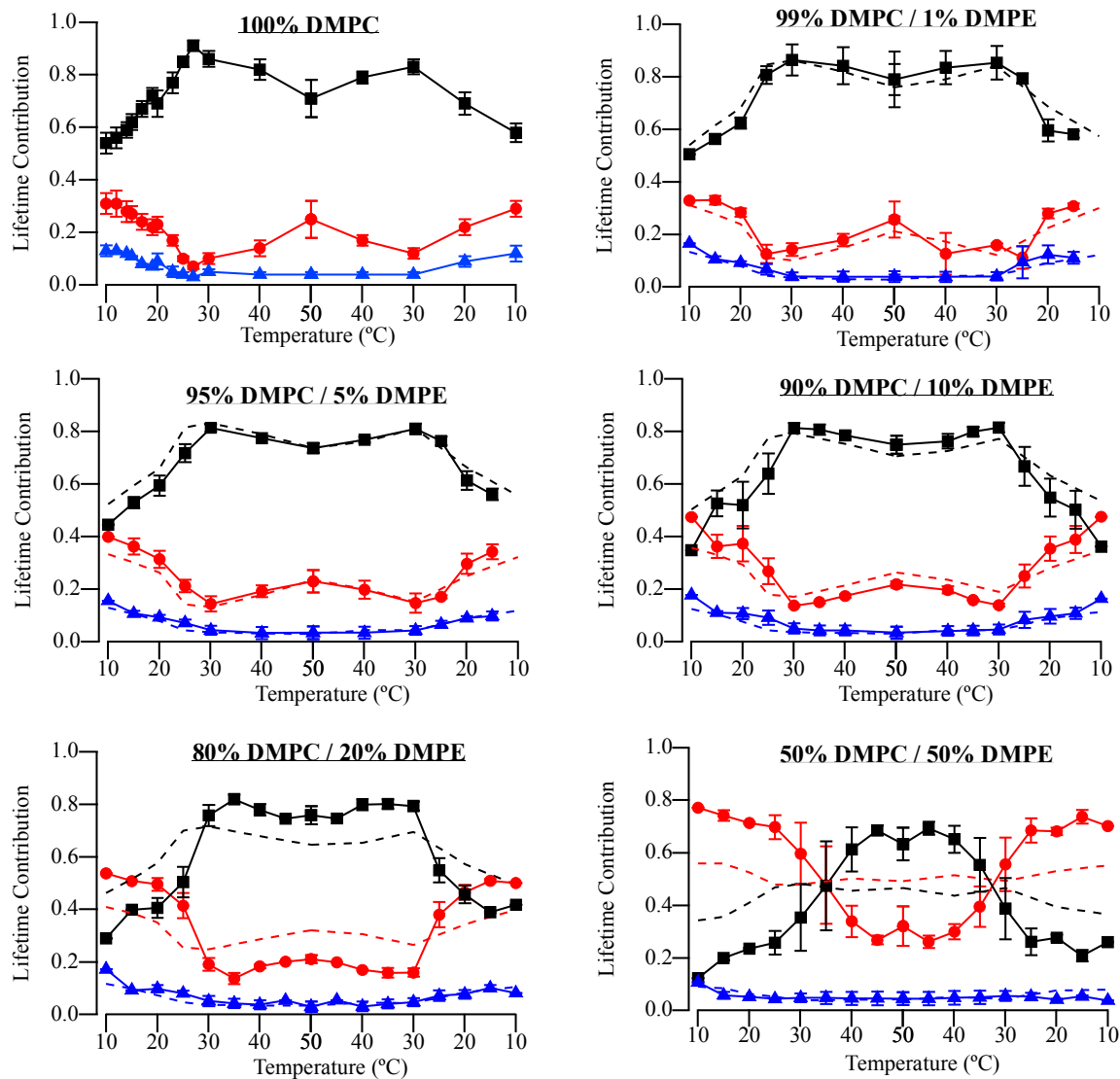


Figure S5. Lifetime contribution of C152 in buffer (red circles), polar (black squares), and nonpolar (blue triangles) environments in vesicles composed of pure DMPC (top left), 99% DMPC/ 1% DMPE (top right), 95% DMPC/ 5% DMPE (middle left), 90% DMPC/ 10% DMPE (middle right), 80% DMPC/ 20% DMPE (bottom left), and 50% DMPC/ 50% DMPE (bottom right).

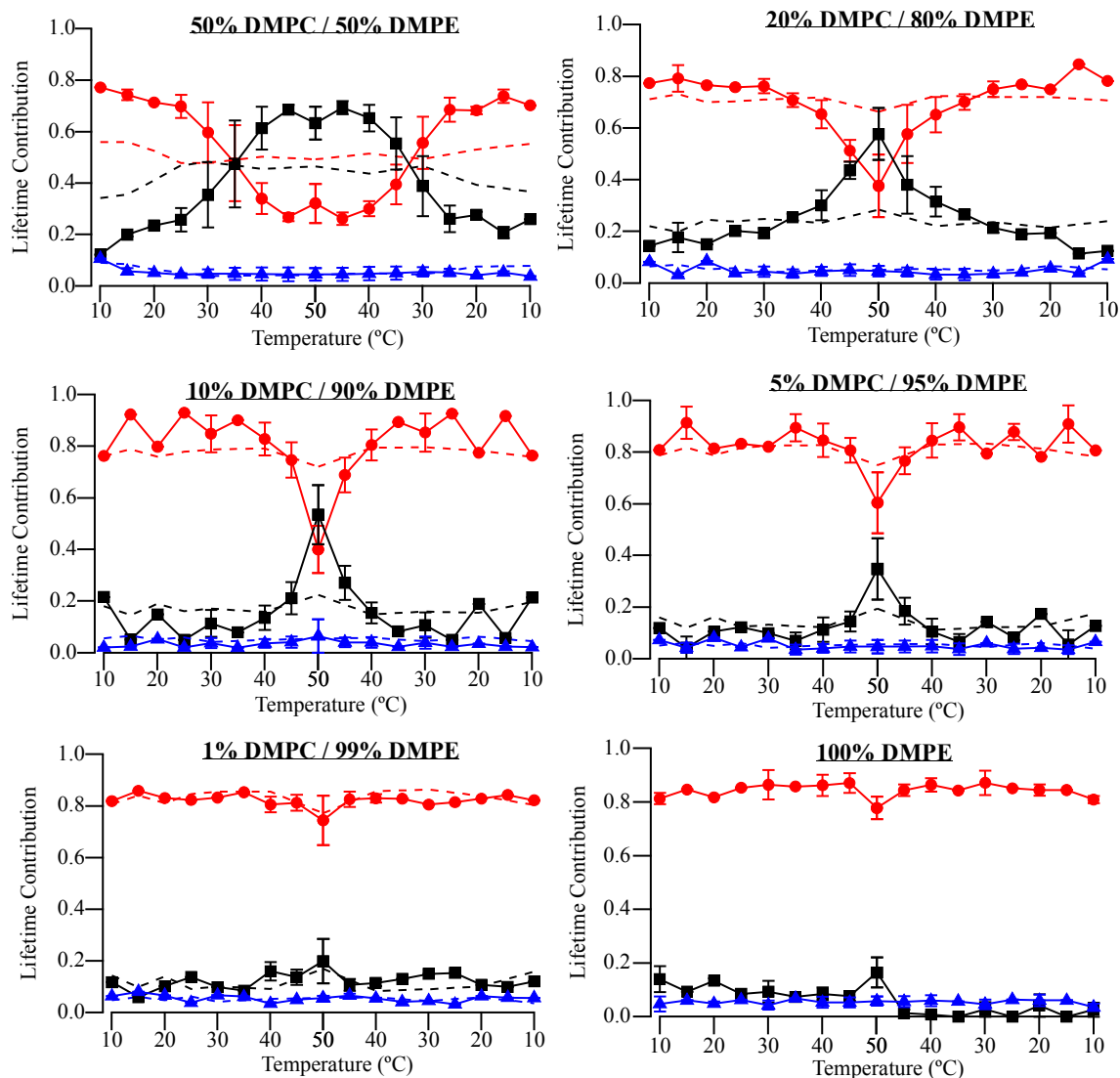


Figure S6. Lifetime contribution of C12 in buffer (red circles), polar (black squares), and nonpolar (blue triangles) environments in vesicles composed of 50% DMPE/ 50% DMPC (top left, equimolar concentration is reshown here for comparison purposes), 80% DMPE/ 20% DMPC (top right), 90% DMPE/ 10% DMPC (middle left), 95% DMPE/ 5% DMPC (middle right), 99% DMPE/ 1% DMPC (bottom left), and pure DMPE (bottom right).

Table S3. Percent of C152 in the buffer, polar, and nonpolar regions of vesicles composed of DLPC, DMPC, and mixtures of the DLPC and DMPC.

<b>DLPC:DMPC</b>	<b>Temp. (°C)</b>	<b>%C152: Buffer</b>	<b>% C152: Polar</b>	<b>%C152: Nonpolar</b>
Pure DLPC (n=4)	10	7 ± 2	78 ± 5	15 ± 5
	20	11 ± 1	85 ± 2	4 ± 1
	30	14 ± 1	82 ± 2	3 ± 1
90 DLPC: 10 DMPC (n=4)	10	13 ± 3	77 ± 8	10 ± 7
	20	15 ± 4	82 ± 5	3 ± 1
	30	19 ± 4	79 ± 4	2 ± 1
80 DLPC: 20 DMPC (n=3)	10	7 ± 2	87 ± 4	6 ± 2
	20	13 ± 5	85 ± 5	2 ± 1
	30	17 ± 6	81 ± 6	2 ± 1
50 DLPC: 50 DMPC (n=4)	10	22 ± 6	61 ± 11	16 ± 5
	20	18 ± 6	76 ± 8	6 ± 3
	30	21 ± 7	75 ± 8	4 ± 3
20 DLPC: 80 DMPC (n=3)	10	27 ± 6	64 ± 1	8 ± 4
	20	20 ± 5	76 ± 3	4 ± 2
	30	16 ± 5	82 ± 5	2 ± 1
10 DLPC: 90 DMPC (n=3)	10	29 ± 4	56 ± 3	14 ± 3
	20	21 ± 3	72 ± 3	7 ± 2
	30	9 ± 4	88 ± 4	3 ± 1
Pure DMPC (n=7)	10	31 ± 4	54 ± 4	13 ± 2
	20	23 ± 3	69 ± 5	5 ± 2
	30	9 ± 2	87 ± 3	4 ± 2

Table S4. Percent of C152 in the buffer, polar, and nonpolar regions of vesicles composed of DLPC, DMPC, and mixtures of the DLPC and DMPC.

<b>DMPC:DMPE</b>	<b>Temp.(°C)</b>	<b>%C152: Buffer</b>	<b>% C152: Polar</b>	<b>%C152: Nonpolar</b>
Pure DMPC (n=7)	10	31 ± 4	54 ± 4	13 ± 2
	20	23 ± 3	69 ± 5	5 ± 2
	30	9 ± 2	87 ± 3	4 ± 2
	50	25 ± 7	71 ± 7	4 ± 1
90 DMPC: 10 DMPE (n=3)	10	47 ± 1	35 ± 1	18 ± 0
	20	37 ± 7	52 ± 9	11 ± 2
	30	14 ± 1	81 ± 2	5 ± 2
	50	22 ± 1	75 ± 3	3 ± 2
80 DMPC: 20 DMPE (n=4)	10	53 ± 1	29 ± 1	17 ± 1
	20	50 ± 2	41 ± 4	10 ± 1
	30	20 ± 2	76 ± 4	5 ± 2
	50	21 ± 1	76 ± 3	3 ± 2
50 DMPC: 50 DMPE (n=3)	10	77 ± 2	12 ± 1	11 ± 1
	20	71 ± 1	23 ± 1	5 ± 1
	30	60 ± 12	35 ± 13	5 ± 2
	50	32 ± 8	66 ± 6	6 ± 2
20 DMPC: 80 DMPE (n=3)	10	77 ± 5	14 ± 6	8 ± 1
	20	77 ± 1	15 ± 1	8 ± 1
	30	76 ± 3	19 ± 2	4 ± 2
	50	38 ± 12	58 ± 10	5 ± 2
10 DMPC: 90 DMPE (n=4)	10	76 ± 1	22 ± 1	2 ± 1
	20	80 ± 1	15 ± 1	5 ± 1
	30	85 ± 7	11 ± 5	4 ± 2
	50	40 ± 10	54 ± 11	6 ± 6
Pure DMPE (n=7)	10	82 ± 2	14 ± 5	5 ± 3
	20	82 ± 1	13 ± 1	5 ± 1
	30	86 ± 5	10 ± 5	4 ± 2
	50	78 ± 4	16 ± 6	6 ± 2